Korean J. Chem. Eng., **29**(8), 1010-1018 (2012)
DOI: 10.1007/s11814-011-0277-0

Model prediction of non-symmetric normal stresses under oscillatory squeeze flow

Jae Hee Kim, Kyung Hyun Ahn†, and Seung Jong Lee

School of Chemical and Biological Engineering, Seoul National University, Seoul 151-744, Korea
(*Received 5 September 2011 • accepted 25 October 2011*)

Abstract–The non-symmetric responses of normal stresses in oscillatory squeeze flow have been investigated with model calculations. The simplest and most widely used constitutive equations were employed to predict the non-symmetric normal stresses, which is a distinctive feature of oscillatory squeeze flow. The model prediction was compared with experimental data of polymer solution in terms of stress shape, Lissajous plot, stress decomposition, and Fourier transformation. The upper-convected Maxwell, Giesekus, and exponential Phan-Thien Tanner models predicted the non-symmetric characteristics of normal stresses under oscillatory squeeze flow. The predictions showed fairly good agreement with experimental data. However, the upper-convected Maxwell model showed unrealistic result in the Lissajous plot of [stress vs. strain] and [stress vs. strain rate]. From stress decomposition, it could be confirmed that the non-symmetric nature arises from the elastic contribution of the normal stress, which was verified in both experiment and model calculation. This study is expected to provide useful insights for further understanding of the nonlinear and non-symmetric characteristics of oscillatory squeeze flow.

Key words: Oscillatory Squeeze Flow, Non-symmetric Stress, Normal Stress, Stress Decomposition

INTRODUCTION

Oscillatory squeeze flow (OSF) has been studied for many years not only in experiment but also in simulation, though less attention has been paid than standard viscometric flow. This flow suffers from transient and inhomogeneous flow field due to the changing flow geometry during oscillation. Nevertheless, oscillatory squeeze flow can be a useful tool to characterize the rheology of complex fluids: adhesives, printing inks, bone joints, biological materials, dental composites, etc. [1-5]. Phan-Thien (1980) established the theoretical background on oscillatory squeeze flow [6]. In experiments, the linear viscoelasticity of viscoelastic fluids under small amplitude oscillatory squeeze flow was examined [2,7]. Numerical simulations have been performed to compare with experimental results. There used to be a major issue in identifying an appropriate rheological model when a simulation was carried out to validate experimental results. A few papers have been published on modeling and simulation of oscillatory squeeze flow. The theoretical analysis with an electrorheological (ER) fluid was performed under oscillatory squeeze flow [8]. A model simulation, using a combination of upper-convected Maxwell (UCM) and Mooney model, was carried out to predict the behavior of viscoelastic fluids in oscillatory squeeze flow [9]. Phan-Thien et al. (2000) also compared experimental results of a biological material that is highly shear thinning with model prediction [3]. Numerical simulation of oscillatory squeeze flow was also performed by employing the finite element method [10]. They identified the strain limit for linear viscoelasticity at varying plate gap and frequency. Although there is useful information in the literature on the rheological characteristics under OSF, there was no concern on the non-symmetric characteristics of normal stress, which is a distinctive feature of oscillatory squeeze flow at larger strain amplitude. The non-symmetric normal stress results from the different response between compression and extension during the oscillation.

The objective of this study is to predict and interpret the non-symmetric stress responses under oscillatory squeeze flow via model simulation and to compare the results with experimental data. Then we will examine the predictability of the constitutive equations. The paper is organized as follows. First, we introduce the theoretical background used in this study including kinematics and constitutive equations. Then, we will show the stress curve, Lissajous plot, and Fourier transform of model predictions from UCM, Giesekus, and PTT model and compare the results with experimental data.

THEORETICAL BACKGROUND

1. Oscillatory Squeeze Flow (OSF)

In dynamic oscillatory squeeze flow, if the imposed frequency is ω, the imposed strain, the strain rate, and the measured normal stress can be defined as follows:

$$\gamma_z(t) = \gamma_{z0}\sin\omega t, \tag{1}$$

$$\dot{\gamma}_z(t) = \gamma_{z0}\,\omega\cos\omega t, \tag{2}$$

$$\sigma_{zz}(t) = \sigma_0\sin(\omega t + \delta_z), \tag{3}$$

where γ_{z0} and σ_0 are the amplitudes of strain and stress, respectively, and δ_z is their phase lag. The schematic diagram of the flow geometry is shown in Fig. 1. The strain amplitude in vertical direction is defined by

$$\gamma_{z0} = \frac{a}{H_0}, \tag{4}$$

where H_0 is the initial gap height, a is the amplitude in vertical motion.

In the linear regime, the dynamic moduli E', E'' and the complex viscosity η^* can be determined as follows:

†To whom correspondence should be addressed.
E-mail: ahnnet@snu.ac.kr

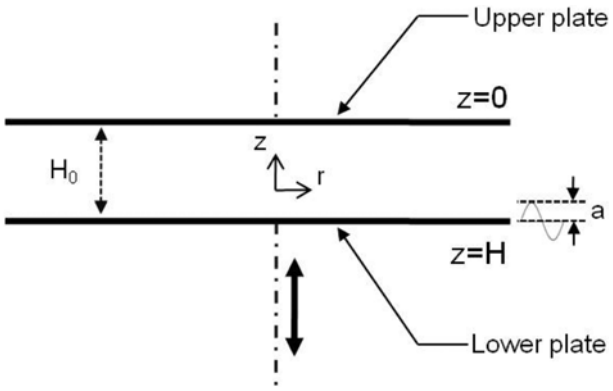

Fig. 1. Schematic diagram of oscillatory squeeze flow between two parallel plates.

$$E' = \frac{2H_0^2}{3R^2}\frac{\sigma_0}{\gamma_{z0}}\cos\delta_z, \tag{5}$$

$$E'' = \frac{2H_0^2}{3R^2}\frac{\sigma_0}{\gamma_{z0}}\sin\delta_z, \tag{6}$$

$$\eta^* = \frac{1}{\omega}\sqrt{(E')^2+(E'')^2}, \tag{7}$$

where R is the radius of the plate [7].

2. Constitutive Equations

Three different constitutive equations of Maxwell type have been employed to predict the nonlinear responses of viscoelastic fluids under oscillatory squeeze flow: upper-convected Maxwell, Giesekus, and exponential Phan-Thien Tanner model with single mode. The simplest model, the upper-convected Maxwell (UCM) model is given by:

$$\tau+\lambda\tau_{(1)}=2\lambda G\mathbf{D} \tag{8}$$

where $\boldsymbol{\tau}$ is the extra-stress tensor, λ and G are the relaxation time and the modulus of the fluid, **D** is the rate of deformation tensor. The subscript (1) denotes the upper convective time derivative, which is defined as follows:

$$\tau_{(1)} = \frac{\partial\tau}{\partial t}+\mathbf{v}\cdot\nabla\tau-(\nabla\mathbf{v})^T\cdot\tau-\tau\cdot\nabla\mathbf{v}. \tag{9}$$

This simple constitutive equation is nonlinear because $\boldsymbol{\tau}_{(1)}$ contains products of the velocity gradient and the stress tensor $\boldsymbol{\tau}$.

We also performed simulation with the Giesekus model,

$$\tau+\lambda\tau_{(1)}+\frac{\alpha}{G}\tau\cdot\tau=2\lambda G\mathbf{D}, \tag{10}$$

where λ and G are the relaxation time and the modulus, **D** is the rate of deformation tensor [11]. The Giesekus model is equivalent to a dumbbell model with anisotropic drag from the viewpoint of kinetic theory. α is the anisotropy parameter or mobility factor which is associated with anisotropic Brownian motion and anisotropic hydrodynamic drag, and typically ranges from 0 to 1. When α=0, this model becomes the upper-convected Maxwell (UCM) model. As α increases, the anisotropic drag becomes more pronounced.

The exponential Phan-Thien Tanner (EPTT) model is given as follows:

$$\tau\exp\left(\frac{\varepsilon}{G}\mathrm{tr}\,\tau\right)+\lambda\tau_{(1)}+\lambda\xi(\mathbf{D}\cdot\tau+\tau\cdot\mathbf{D})=2\lambda G\mathbf{D}. \tag{11}$$

Here, λ and G are the relaxation time and the modulus, **D** is the rate of deformation tensor. This model was derived based on a network theory which includes non-affine motion [11]. ξ and ε are the nonlinear parameters, which control the level of shear thinning. If $\xi\neq0$, unphysical oscillation occurs in the prediction of steady shear viscosity and first normal stress coefficient during the start-up of shear flow. When ξ is set to zero, the motion is supposed to be affine; the unphysical oscillation disappears but shear thinning still exists due to the nonlinear parameter, ε. Thus, we performed model simulations with ξ=0, and varied ε from 0 to 1. As the nonlinear parameter ε increases, the level of shear-thinning becomes pronounced in shear flow.

EXPERIMENTAL PROCEDURE

The oscillatory squeeze experiment was performed on a conventional rheometer (RMS, TA Instruments) with a modified fixture [18]. In the oscillatory squeeze flow mode, the fluid is held between two parallel-plates (diameter: upper plate 40 mm and lower plate 50 mm; initial gap: 1.5 mm). The top plate is stationary, while the bottom plate is subjected to dynamic motion in vertical direction only. The normal stress was measured by a transducer connected

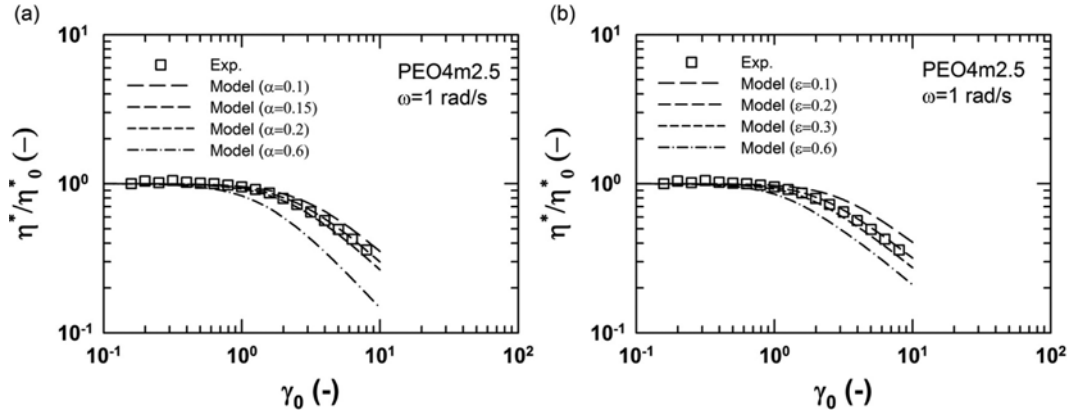

Fig. 2. Reduced shear viscosity from experiment (symbols) and simulation (dashed lines) at ω=1 rad/s: (a) Giesekus model, (b) exponential PTT (EPTT) model, at various nonlinear parameters.

to the upper fixture, and recorded by an on-line computer. Polyethylene oxide solution (PEO, Sigma-Aldrich) was used as a viscoelastic fluid that is highly shear-thinning. Silicone oil was used to prevent evaporation of PEO aqueous solutions at the edge disclosed to the air. For raw data acquisition, a 16bit ADC card (PCI-6052E; National Instruments) with sampling rate up to 100 kHz was used. The normal stress and strain data were recorded simultaneously by the ADC card which was plugged into a personal computer. All measurements were taken at room temperature.

RESULTS AND DISCUSSION

1. Model Parameters

We set the nonlinear parameters by comparing model prediction to experimental data from the dynamic strain sweep test under simple shear flow. The relative viscosity (η^*/η_0^*) is plotted as a function of strain amplitude at specified nonlinear parameters (α, ε) in Fig. 2. As the nonlinear parameter α for Giesekus model and ε for EPTT model increases, strain-thinning behavior becomes more pronounced. When α=0.15 for Giesekus model and ε=0.2 for EPTT model, the reduced viscosity best fits with experimental data. Although the

Table 1. Description of the sample used. Zero-shear viscosity (η_0^*) was obtained by fitting the complex viscosity data to the Carreau model*. The relaxation time (λ) is the reciprocal of the cross-over frequency [ω_c, frequency at $G'(\omega)=G''(\omega)$ in the frequency sweep test]

Sample	Molecular weight	Concentration (wt%)	η_0^* (Pa·s)	G_0 (Pa)	λ ($=1/\omega_c$)
PEO4m2.5	4×10^6	2.5	114	104	1.1

*Carreau model: $\eta/\eta_0=[1+(a\dot{\gamma})^b]^{(n-1)/b}$

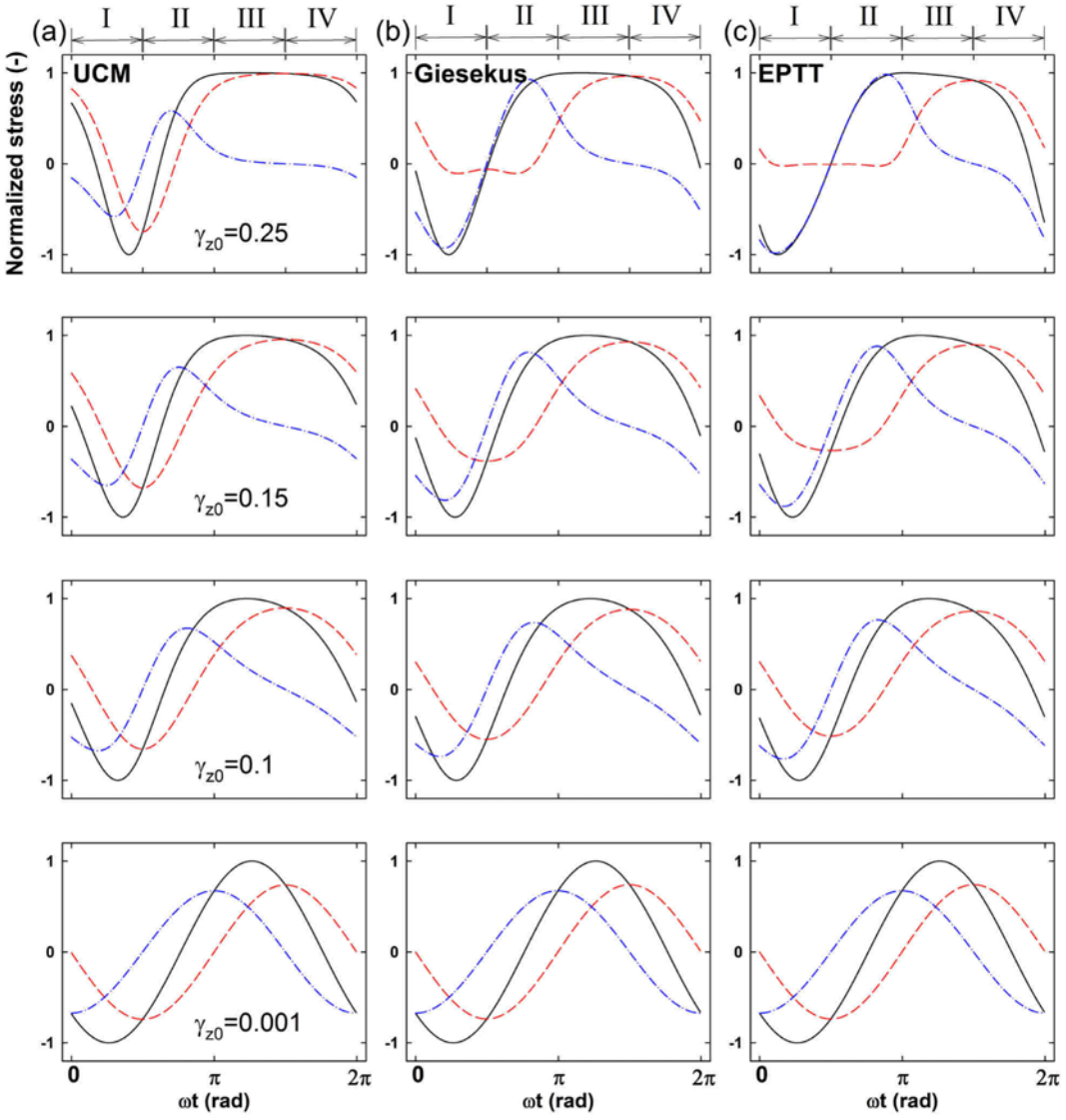

Fig. 3. Normal stress (solid line), elastic stress (dashed line), and viscous stress (dashed-dot line); (a) UCM model (G=104, λ=1.1), (b) Giesekus model (α=0.15, G=104, λ=1.1), (c) EPTT model (ε=0.2, ξ=0, G=104, λ=1.1) at frequency 1 rad/s. The elastic and viscous stresses were obtained from stress decomposition (SD). The indices I and IV indicate compression; II and III indicate extension during oscillation.

nonlinear parameters were determined by fitting with viscosity in shear flow, it will be used in numerical simulations for oscillatory squeeze flow [10]. Table 1 lists the characteristics of the samples used in this work.

2. Stress Curve and Lissajous Plot

To investigate the nonlinear response of normal stresses under oscillatory squeeze flow, we performed model simulations employing the UCM model, Giesekus model, and EPTT model. To analyze the normal stress signals, stress shape analysis, Lissajous plot analysis, and stress decomposition (SD) have been performed. Stress shape analysis shows the raw stress signal, which varies from sinusoidal to distorted wave as the strain amplitude increases. The stress shape provides insightful and visual information during structural changes of the material when the deformation becomes large. The Lissajous plot, which is plotted as [stress vs. strain] or [stress vs. strain rate], is useful in observing the transformation of nonlinear responses. The Lissajous plot is elliptical in the linear regime, but becomes distorted in the non-linear regime. Stress decomposition (SD) separates the nonlinear stress response into elastic and viscous contributions using symmetric arguments [12-14]. The decomposition is based on the idea that elastic stress (σ') should be an odd function of strain and even function of strain rate, while viscous stress (σ'') should be even in strain and odd in strain rate. Fig. 3 shows the normal stress, elastic stress, and viscous stress calculated from the UCM model, Giesekus model with α=0.15, and EPTT model with ε=0.2, ξ=0 for G=104, λ=1.1. The normal stress was normalized by its amplitude. The normal stress changes from sinusoidal to distorted shape, and from symmetric to non-symmetric shape with respect to zero mean value as the strain amplitude increases as shown in Fig. 3. This non-symmetric response is one of the distinctive features of the normal stresses under oscillatory squeeze flow [3,9]. The constitutive equations show a non-linear and non-symmetric response under oscillatory squeeze flow in the simple model prediction. By stress decomposition (SD), we can get addi-

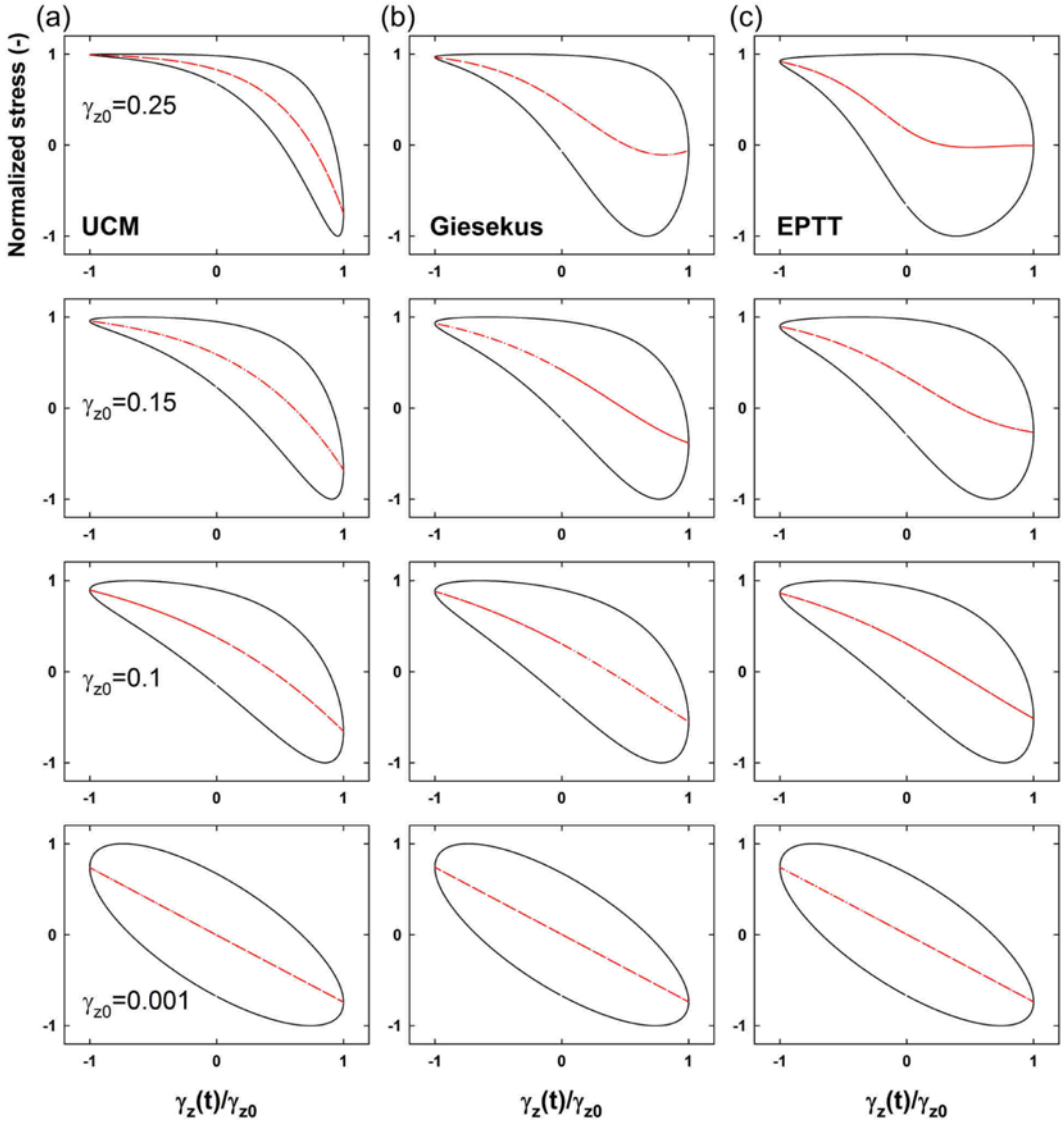

Fig. 4. Closed loops are normal stress vs. strain, [$\sigma_{zz}(t)/\sigma_0$ vs. $\gamma_z(t)/\gamma_{z0}$], and dotted lines are elastic stress vs. strain, [$\sigma'_{zz}(t)/\sigma_0$ vs $\gamma_z(t)/\gamma_{z0}$]; (a) UCM model (G=104, λ=1.1), (b) Giesekus model (α=0.15, G=104, λ=1.1), (c) EPTT model (ε=0.2, ξ=0, G=104, λ=1.1) at frequency 1 rad/s. The elastic and viscous stresses were obtained from stress decomposition (SD).

tional information on the non-symmetric response of normal stress under OSF. For all the constitutive equations we have considered, the elastic and viscous stresses are sinusoidal at low strain amplitude, which means linear viscoelasticity. As the strain amplitude increases, the elastic and viscous stresses show distorted shape, which means non-linear viscoelasticity, but they show different stress shape. At larger strain amplitude, the elastic stress shows non-symmetric response in both positive and negative region, but the viscous stress displays symmetric response. Furthermore, the elastic stress shows a difference in magnitude at maximum and minimum, while the viscous stress does not show any significant difference. Therefore, it can be known that the non-symmetric stress signal arises mainly from the elastic contribution in the normal stress.

The Lissajous plots ([stress vs. strain] and [elastic stress vs. strain]) are displayed in Fig. 4. The loop of [stress vs. strain] and [elastic stress vs. strain] shows different shape at larger strain amplitude according to the constitutive equations. The loop of [stress vs. strain] varies from symmetric to non-symmetric shape with respect to zero mean value as the strain amplitude increases. At low strain amplitude 0.001, the loop of [stress vs. strain] is symmetric, which is caused by the same response of the fluid during compression and extension. However, at higher strain amplitudes, the loops become non-symmetric, which implies different response during the oscillation. As the strain amplitude increases, this non-symmetric response becomes more pronounced in all predictions as shown in Fig. 4. The internal area of the loop corresponds to the mechanical energy dissipation, and normally increases with strain amplitude, that is, mechanical energy dissipation $\approx(\omega/\pi\gamma_{z0}^2)|\oint\sigma_{zz}\,d(\gamma_z)|$. The Giesekus and EPTT models show that the area increases with strain amplitude, while that of UCM model decreases with strain amplitude. In this sense, the UCM model exhibits poor prediction under oscillatory squeeze flow. At small strain amplitude 0.001, the elastic Lissajous plot of [elastic stress vs. strain] shows a straight line, which means linear response. On the other hand, as the strain amplitude increases,

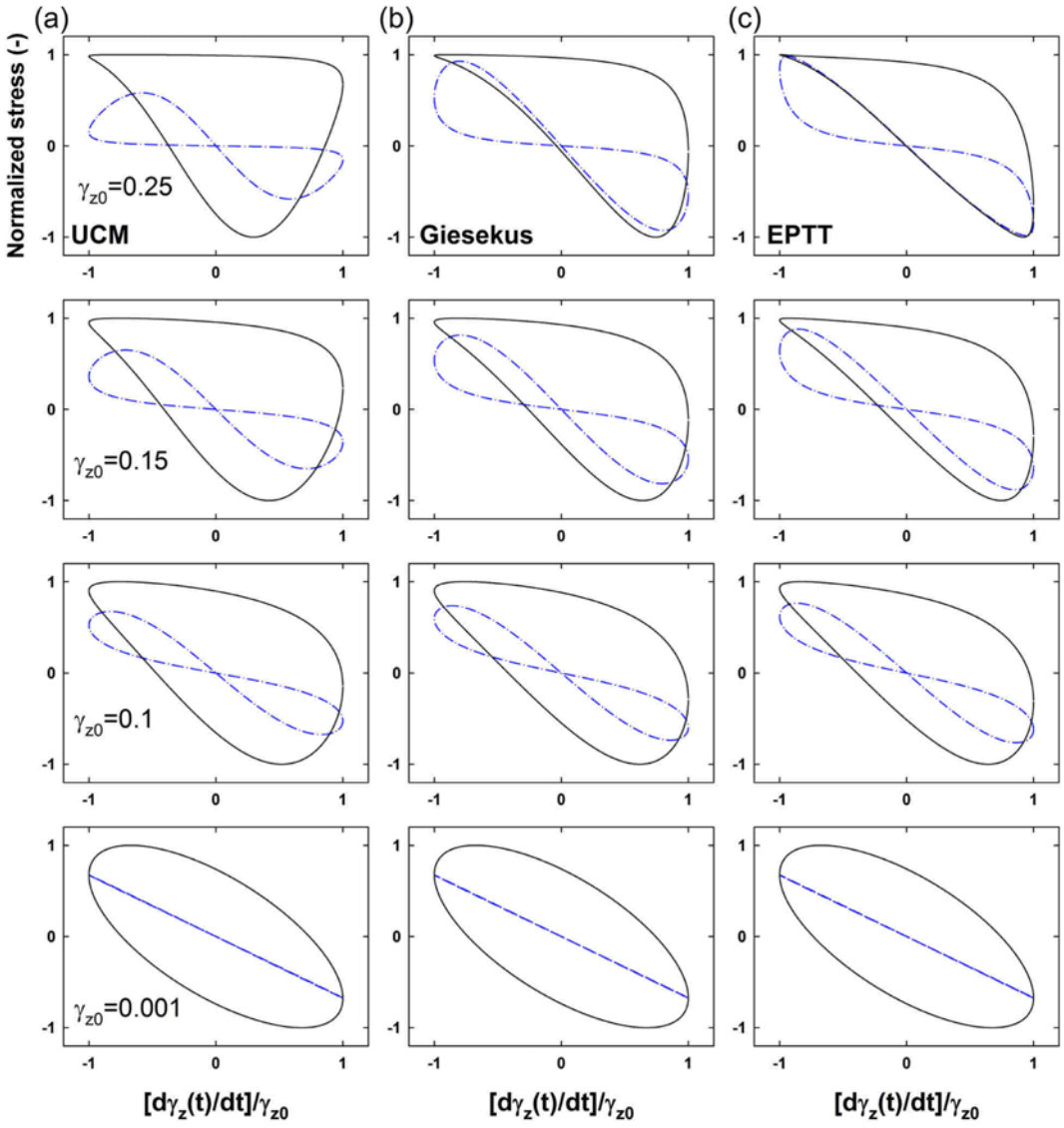

Fig. 5. Closed loops are normal stress vs. strain rate, $[\sigma_{zz}(t)/\sigma_0$ vs. $\dot{\gamma}_z(t)/\gamma_0]$, and dashed lines are viscous stress vs. strain rate, $[\sigma''_{zz}(t)/\sigma_0$ vs. $\dot{\gamma}_z(t)/\gamma_0]$; (a) UCM model (G=104, λ=1.1), (b) Giesekus model (α=0.15, G=104, λ=1.1), (c) EPTT model (ε=0.2, ξ=0, G=104, λ=1.1) at frequency 1 rad/s. The elastic and viscous stresses were obtained from stress decomposition (SD).

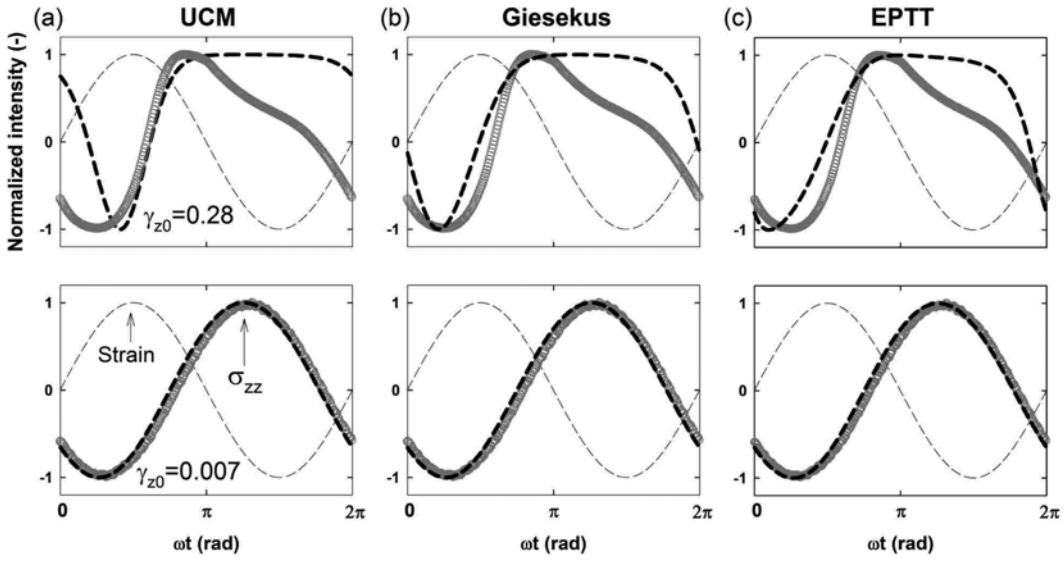

Fig. 6. Normal stress; (a) UCM model, (b) Giesekus model (α=0.15), (c) EPTT model (ε=0.2, ξ=0) for G=104, λ=1.1. The experimental data (PEO4m2.5, symbols) are compared with model predictions (thick lines) at frequency 1 rad/s. The strain (thin lines) is plotted together as a reference.

the straight line of elastic stress becomes non-symmetric curvilinear, which means nonlinear viscoelasticity under OSF. All model equations show the non-symmetric curvilinear response at larger strain amplitude, as shown in Fig. 4. In general, the elastic Lissajous plot keeps a symmetric curvilinear line even at very large strain amplitude in oscillatory shear flow. This non-symmetric curvilinear line means that the elastic stress is responsible for the non-symmetric characteristics of normal stress in oscillatory squeeze flow.

Fig. 5 shows the loops of both [stress vs. strain rate] and [viscous stress vs. strain rate] at various strain amplitudes. The loop of [stress vs. strain rate] changes from elliptic to distorted shape and becomes non-symmetric with the increase of strain amplitude. The elliptical and symmetric shapes result from the same response during compression and extension. But, the distorted and non-symmetric shapes are caused by the different response during the oscillation. The constitutive equations show similar results in the Lissajous plot at low strain amplitude, but exhibit a different shape at larger strain amplitude. At large strain amplitude γ_{z0}=0.25, the UCM model shows an unrealistic result, in which the area of the [stress vs. strain rate] loop is nearly constant, independent of strain amplitude. The area of the loop [stress vs. strain rate] corresponds to the mechanical energy storage, that is, mechanical energy storage$\approx(\omega/\pi\gamma_{z0}^2)|\oint\sigma_{zz}\,d(\dot{\gamma}_z/\omega)|$. In general, the area of [stress vs. strain rate] loop decreases with strain amplitude [15,16]. On the other hand, the Giesekus model and EPTT model show a reasonable result, in which the area of the loop decreases as the strain amplitude increases. The Lissajous plot of [viscous stress vs. strain rate] changes from a straight line to a one-fold loop as the strain amplitude increases. The straight line indicates a linear response, but the one-fold loop represents a nonlinear response during oscillation. The one-fold loop is a unique feature of oscillatory squeeze flow that results from the difference in normal stress responses during compression and extension. All model equations predicted this one-fold symmetric loop, as shown in Fig. 5. This behavior has never been observed in large amplitude oscillatory shear (LAOS), which has a symmetric loop for the viscous stress [13]. The one-fold loop of [viscous stress vs. strain rate] keeps the symmetric response with respect to zero mean value, even at larger strain amplitude. The symmetry in the viscous Lissajous plot indicates that the viscous stress contributes little to the non-symmetric characteristics of the normal stresses in OSF. From the Lissajous plots of elastic and viscous stresses, it can be confirmed that the non-symmetric nature of normal stresses in OSF originates from the elastic contribution, not from the viscous contribution.

We compared experimental data of PEO solution (PEO4m2.5) with simulation results calculated by UCM model, Giesekus model (α=0.15), and EPTT model (ε=0.2, ξ=0). The normal stresses are plotted as a function of time in Fig. 6. The stress curve varies from sinusoidal to distorted, and changes from symmetric to non-symmetric at both positive and negative region. At low strain amplitude, the predictions are good, while the predictions are poor at larger strain amplitude. The models predict the non-symmetric stresses very well, but show a large deviation in a quantitative sense, especially at the positive region over the x-axis. The deviation of the UCM model is larger than that of the Giesekus and EPTT models. The discrepancy comes partly from the broad spectrum of relaxation modes in the polymer solution (the models are all single mode), but may originate from the incompleteness of the constitutive equations. In this sense, the oscillatory squeeze flow can be a good test flow to evaluate the performance of the constitutive equations.

Fig. 7 shows the Lissajous plot of [stress vs. strain] and [elastic stress vs. strain] at strain amplitudes, 0.007 and 0.28. At small strain amplitude 0.007, both the loop of [stress vs. strain] and [elastic stress vs. strain] display elliptical and straight line, respectively, which indicates linear viscoelasticity. However, the plot of [stress vs. strain] exhibits a non-symmetric loop at larger strain amplitude, and the plot of [elastic stress vs. strain] shows a non-symmetric curvilinear curve, in both experiment and model predictions. In this sense, the model equations qualitatively predict non-symmetric characteristics of normal stress reasonably well. However, the predictions are far from realistic in the quantitative sense. The non-symmetric curvi-

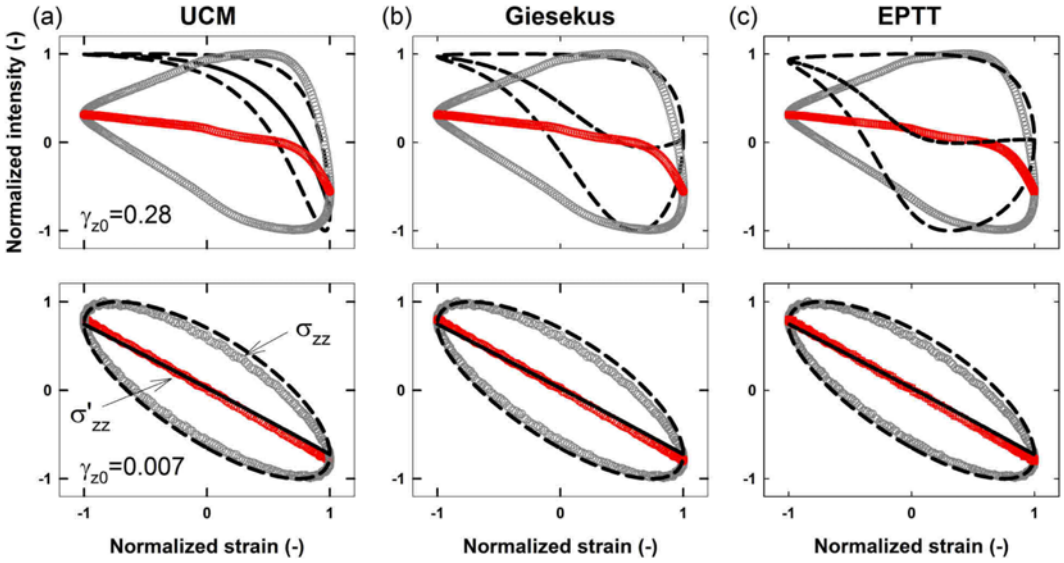

Fig. 7. Lissajous plot of normal stress vs. strain, [$\sigma_{zz}(t)/\sigma_0$ vs. $\gamma_z(t)/\gamma_{z0}$], and elastic stress vs. strain, [$\sigma'_{zz}(t)/\sigma_0$ vs $\gamma_z(t)/\gamma_{z0}$]; (a) UCM model, (b) Giesekus model (α=0.15), (c) EPTT model (ε=0.2, ξ=0) for G=104, λ=1.1. The experimental data (PEO4m2.5, symbols) are compared with model predictions (dashed lines) at frequency 1 rad/s.

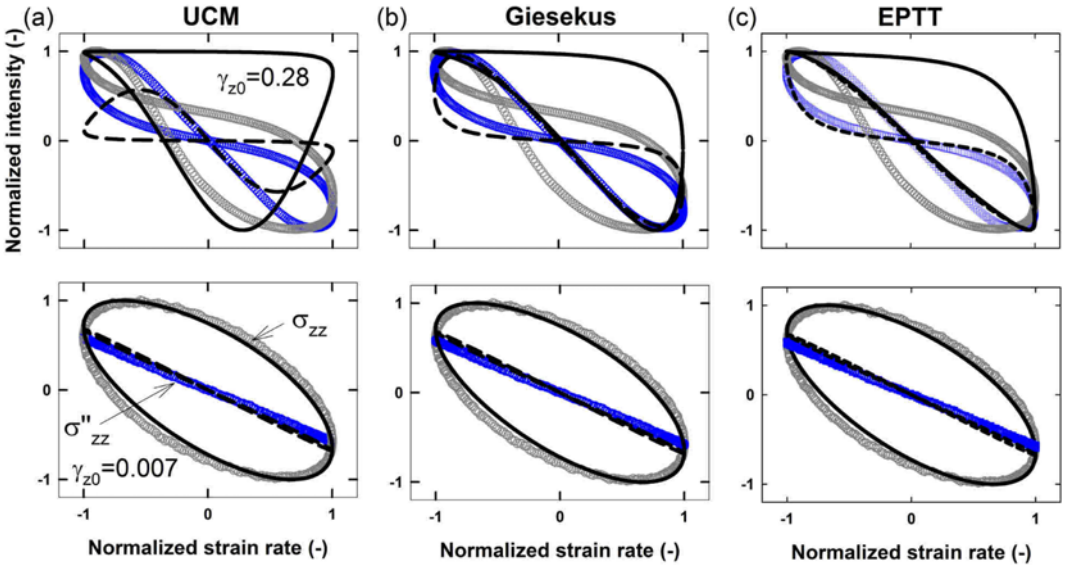

Fig. 8. Lissajous plot of normal stress vs. strain rate, [$\sigma_{zz}(t)/\sigma_0$ vs. $\dot{\gamma}_z(t)/\dot{\gamma}_{z0}$] and viscous stress vs. strain rate, [$\sigma''_{zz}(t)/\sigma_0$ vs. $\dot{\gamma}_z(t)/\dot{\gamma}_{z0}$]; (a) UCM model, (b) Giesekus model (α=0.15), (c) EPTT model (ε=0.2, ξ=0) for G=104, λ=1.1. The experimental data (PEO4m2.5, symbols) are compared with the model prediction (lines) at frequency 1 rad/s.

linear curve means that the elastic stress is responsible for the non-symmetric response of normal stress during oscillation, which includes both compression and extension.

We also plotted [stress vs. strain rate] and [viscous stress vs. strain rate] in Fig. 8. At strain amplitude 0.007, the curves of both [stress vs. strain rate] and [viscous stress vs. strain rate] show elliptical shape and straight line, respectively, which means linear response. However at high strain amplitude 0.28, the loop of [stress vs. strain rate] shows one-fold non-symmetry in experiment only and the loop of [viscous stress vs. strain rate] displays one-fold symmetry in both experiment and model predictions. Both one-fold non-symmetric and one-fold symmetric loops mean the non-linear response. Unlike elastic stress, the viscous stress keeps symmetry from small to large strain amplitudes. Our model predictions show good agreement with experiment in the loop of [viscous stress vs. strain rate] except UCM model. However, all model predictions (dashed line) which show non-symmetric loop do not predict one-fold non-symmetric loop of [stress vs. strain rate] observed from experiment. Here again, it is clear that the oscillatory squeeze flow can be a good test flow to evaluate the performance of the constitutive equations. From this viscous Lissajous plot showing one-fold symmetry, it is confirmed that the viscous stress is not related to the non-symmetry of normal stress in both experiment and model predictions.

In comparison with experiment, our model simulation showed

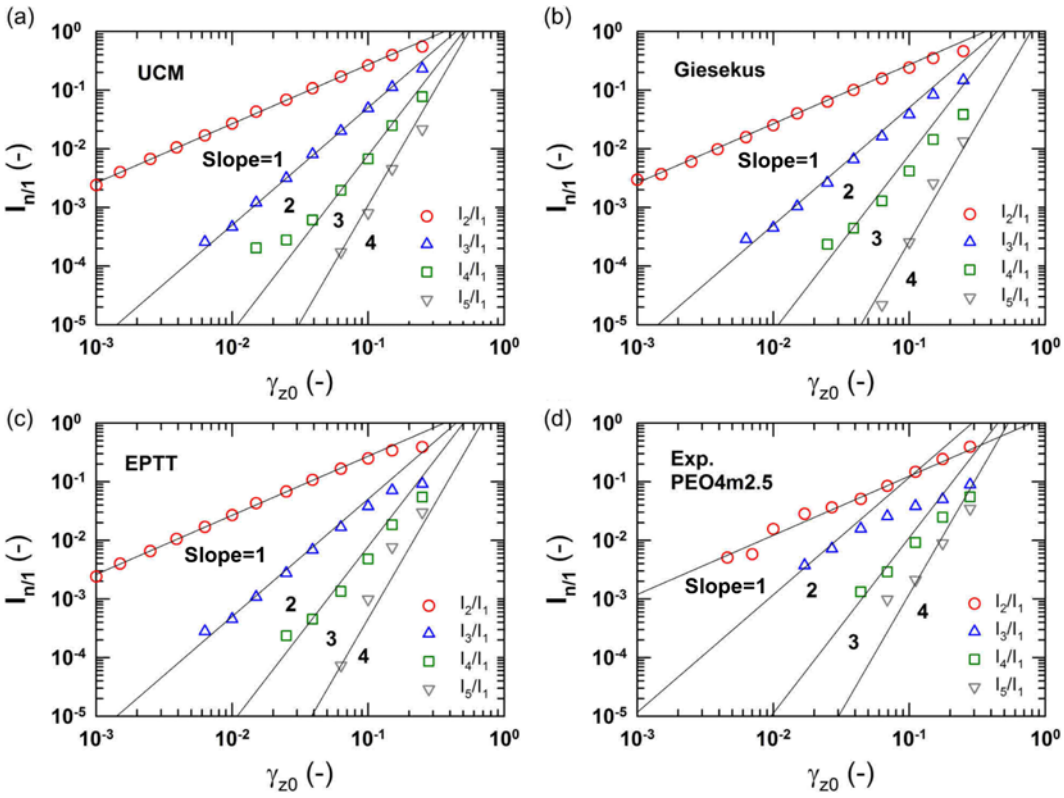

Fig. 9. Relative Fourier intensity ($I_{n/1}$) as a function of strain amplitude; (a) UCM model (G=104, λ=1.1), (b) Giesekus model (α=0.15, G=104, λ=1.1), (c) EPTT model (ε=0.2, ξ=0, G=104, λ=1.1), (d) experimental data of PEO4m2.5, at frequency 1 rad/s. The lines indicate linear fitting with Eq. (12).

good prediction in terms of the non-symmetric stress signal and corresponding Lissajous plot except the UCM model. However, the model predictions fail to describe the experimental data completely. A possible cause of the discrepancy lies in determining the set of nonlinear parameters (α, ε). The model prediction is very sensitive to the variation of the non-linear parameters [17]. It may be that the best-fit to the shear viscosity (in Fig. 2) is not the best-fit to the normal stress. The discrepancy can also be explained in terms of the relaxation spectrum of the polymer solution. The polymer solution typically has a broad relaxation spectrum due to its broad molecular weight distribution; however, we considered only the models with single relaxation mode. If multi-mode is considered in model calculation, the discrepancy may be minimized between experiment and simulation. And lastly, we cannot remove the possibility that the constitutive equations are not complete enough to predict the response of viscoelastic fluids under the oscillatory squeeze flow.

3. Fourier Transform (FT) Analysis

Fourier transformation captures the inherent periodic nature of time dependent signals and displays the corresponding amplitudes and phases as a function of frequency. FT is widely used to quantify nonlinearity with high sensitivity. In both experiment and simulation, the normal stress reveals all high order harmonics, both odd and even. The Fourier intensity increases and higher order harmonics start to appear as the strain amplitude increases. The reason why all higher harmonics appear is due to the non-symmetric nature of the normal stresses in the oscillatory squeeze flow. The higher-order harmonic intensity divided by the fundamental intensity, $I_{n/1}$, is plotted as a function of strain amplitude in Fig. 9. The relative intensity $I_{n/1}$ shows a scaling relationship with strain amplitude as follows:

$$\log(I_{n/1})=a+b\log\gamma_{z0} \quad (12)$$

where a is an intercept and b is the slope in the log-log plot. In Fig. 9, the lines indicate linear regression with Eq. (12). $I_{n/1}$ obtained from model equations are almost proportional to the (n-1)th power of strain amplitude. This relationship is similar to that of large amplitude oscillatory shear, in both experiment and simulation [16,17]. In the oscillatory squeeze flow, the relative intensity grows with both odd and even power (b=1, 2, 3, …) of strain amplitude for normal stress. The relative intensity shows similar trend and slope (b) in both experiment and model predictions. The model predictions show good agreement with experiment in terms of FT rheology. Also, the normal stresses calculated from the model equations as well as from experiment all show high order contributions.

CONCLUSIONS

We have predicted the non-symmetric response of normal stresses under oscillatory squeeze flow by model calculation. The UCM, Giesekus, and EPTT models were employed to predict the non-symmetric stress, which is one of the distinctive features of oscillatory squeeze flow. The model prediction was compared with experimental results in terms of stress shape, Lissajous plot, stress decomposition, and Fourier transformation. Furthermore, we examined and

compared the performance of the constitutive equations in terms of non-linear and non-symmetric response under oscillatory squeeze flow. All the constitutive equations predicted the non-symmetric characteristics of normal stresses in nonlinear regime under oscillatory squeeze flow. However, the UCM model displayed unrealistic results such that the mechanical energy storage is nearly constant and the mechanical energy loss decreases with strain amplitude. In both experiment and simulation, the normal stress changed from sinusoidal to distorted shape, and varied from symmetric to non-symmetric with respect to zero mean value as the strain amplitude increased. By stress decomposition (SD), we found that the elastic stress is non-symmetric with respect to zero mean value at larger strain amplitude and shows difference in magnitude at maximum and minimum. As the strain amplitude increases, the straight line of [elastic stress vs. strain] became non-symmetric curvilinear line, but the loop of [viscous stress vs. strain rate] showed symmetric shape even at larger strain amplitude. From the stress decomposition, it was concluded that the non-symmetric signal arises from the elastic contribution in the normal stress. In comparison with experiment, the models predicted the non-symmetric stresses and corresponding non-symmetric Lissajous loop except for UCM model, but there existed fairly large deviation between model prediction and experiment. They could not predict the one-fold non-symmetric loop in [stress vs. strain rate] at large strain amplitude. A possible cause of the discrepancy lies in determining the set of nonlinear parameters and in considering the relaxation spectrum. In FT analysis, the model prediction showed all high harmonic contributions of both odd and even harmonics, and the relative intensity ($I_{n/1}$) was proportional to the (n-1)th power of strain amplitude in accordance with the experimental data.

ACKNOWLEDGEMENT

This work was supported by the National Research Foundation of Korea (NRF) grant (No. 20100026139) funded by the Korea government (MEST).

REFERENCES

1. J. Kramer, *Appl. Sci. Res.*, **30**, 1 (1974).
2. J. S. Field, M. V. Swain and N. Phan-Thien, *J. Non-Newtonian Fluid Mech.*, **65**, 177 (1996).
3. N. Phan-Thien, S. Nasseri and L. E. Bilston, *Rheol. Acta*, **39**, 409 (2000).
4. P. Jiang, H. See, M. Swain and N. Phan-Thien, *Rheol. Acta*, **42**, 118 (2004).
5. H. See and P. Nguyen, *J. Soc. Rheol., Japan*, **32**, 33 (2004).
6. N. Phan-Thien, *J. Australia Math. Soc. B*, **32**, 22 (1980).
7. D. Bell, D. Binding and K. Walters, *Rheol. Acta*, **46**, 111 (2006).
8. J. Sproston, S. Rigby, E. Williams and R. Stanway, *J. Phys. D: Appl. Phys.*, **27**, 338 (1994).
9. N. Phan-Thien, *J. Non-Newtonian Fluid Mech.*, **95**, 343 (2000).
10. B. Debbaut and K. Thomas, *J. Non-Newtonian Fluid Mech.*, **124**, 77 (2004).
11. R. G. Larson, *Constitutive equations for polymer melts and solutions*, Butterworths, Boston (1988).
12. K. S. Cho, K. Hyun, K. H. Ahn and S. J. Lee, *J. Rheol.*, **49**, 747 (2005).
13. K. S. Cho, K. W. Song and G. S. Chang, *J. Rheol.*, **54**, 27 (2010).
14. K. S. Cho and J. E. Bae, *Korea-Austalia Rheol. J.*, **23**, 49 (2011).
15. R. H. Ewoldt, A. E. Hosoi and G. H. McKinley, *J. Rheol.*, **52**, 1427 (2008).
16. K. Hyun, M. Wilhellm, C. O. Klein, K. S. Cho, J. G. Nam, K. H. Ahn, S. J. Lee, R. H. Ewoldt and G. H. Mckinley, *Prog. Polym. Sci.* (In press) (2011).
17. J. G. Nam, K. Hyun, K. H. Ahn and S. J. Lee, *J. Non-Newtonian Fluid Mech.*, **150**, 1 (2008).
18. J. H. Kim, K. H. Ahn and S. J. Lee, *Rheol. Acta*, (Submitted) (2011).